A Fully 3D Printed Multi-Chip Module with an On-Package Enhanced Dielectric Lens for mm-Wave Applications Using Multimaterial Stereolithography

Ryan Bahr, Xuanke He, Bijan Tehrani, and Manos M. Tentzeris

School of Electrical and Computer Engineering, Georgia Institute of Technology

Email: rbahr3@gatech.edu

Abstract— In the first demonstration of multimaterial stereolithography 3D printing for electromagnetic applications, two 2x2 mm dies of different thicknesses (150 and 200 um) are interconnected with inkjet printing of silver nanoparticle inks (SNP) to form 3-D interconnects. The dies are encapsulated utilizing Stereolithography (SLA) 3-D printing with an acrylate photopolymer resin. A 24.125 GHz right hand circular (RHC) patch antenna is inkjet printed with a novel beam forming ring (BFR) embedded into an integrated hollow dielectric lens of a secondary SLA printed ceramic photopolymer, enabling improved gain and reducing the size while avoiding dielectric loading and losses. The ability to 3-D print multiple materials of different dielectric constants at optical resolutions enables the formations of entirely new structures to be integrated into system-on-package solutions for mm-wave applications.

Index Terms—3D Printing, Additive Manufacturing, Metal Coated Plastics, mm-Wave, Stereolithography, dielectric lens, ceramic, beam forming ring.

I. INTRODUCTION

Additive manufacturing enables low cost, rapid design of new structures and topologies with exotic materials, minimal waste, on-demand controllable dielectric constants and intricate features. A wide assortment of techniques have been in rapid development recently, especially in ways to integrate electronics with conductive multilateral printing. While a variety of 3D printing techniques exist, many have limited multi-material support [1]. Fused deposition modeling (FDM) printing enables the deposition of multiple materials simultaneously through the use of a coexisting direct write system, though the printing resolution and quality are highly dependent on the materials and can be challenging to print consistently and reliably. Stereolithography (SLA) 3D printing enables resolutions that are only limited by optics resulting in smoother prints with greater consistency of successful prints, though requires specific photopolymer resin materials for fabrication.

In this paper, we utilize multi-material stereolithography in order to demonstrate the first multi-dielectric SLA printing for electromagnetic applications [2]. The high resolution 3D SLA printing technique enables feature sizes and surface roughnesses sufficient for next generation mm-Wave and 5G devices thus allowing for the low cost integration of systems and device performance enhancement. The technique is utilized to create a system-on-package (SoP) module with a novel beam-forming ring (BFR) embedded into a hollow dielectric elliptical lens, enabled by the ability to print embedded metallic designs within an SLA print [3]. The print is integrated with encapsulated blank dies to demonstrate the foundational work necessary to create and integrate 3D SoP that enables the ability to create fully printable complete 3D SoP systems. The proposed approach aims in providing the first steps for next-generation 3D printing systems with reduced size and lower cost that will enable varying dielectric constants for gradient materials, distributed Bragg reflectors, improved filter design, antenna efficiency and many more applications where dielectrics lay a key role in design.

II. MULTI-MATERIAL STEREOLITHOGRAPHY PRINTING

Stereolithography printing functions by exposing liquid photopolymer resins to UV light (often 405 nm, corresponding to blu-ray light sources) which crosslinks the polymer with covalent bonds, similar to a positive photoresist, forming isotropic adhesion between layers. There exist two main methods of exposure, laser (SLA) or digital light processing (DLP or DLP SLA) based. Often, laser based systems are simply called SLA, and DLP based systems are considered a subset of SLA systems and often designated as DLP or DLP SLA printing. Laser based systems are more common, utilizing galvanometer mirror systems to steer a beam throughout the build area. The laser-based systems offer larger build areas and higher irradiance versus their DLP counterparts. The two main downsides are that the entire layer needs to be traced similar to FDM printing, and that the beam's cross section expands as the angle of incidence increases, causing a loss in resolution. Typical beam widths are approximately 140 μm (without additional lenses), with the layer height reaching 25 μm and below [4].

DLP based stereolithography, on the other hand, uses a digital micromirror device (DMD) to create a digital mask, exposing an entire layer simultaneously, enabling scalable printing of multiple devices of the same height/layer count without requiring any additional time, identical in function to a maskless aligner used in mask generation in a semiconductor foundry. Often 1080p DMD chips are utilized, and the resolution of a DLP printer is limited by the focal distance which determines the pixel dimensions. The open-source modified DLP-based SLA LittleRP 3D printer was used for the design presented in this paper and was tuned to print with 38 μm features with a build area of 40 mm x 60 mm x 100 mm for the XYZ dimensions, respectively. Tolerances are difficult to characterize with

many 3D printers due to many dependent factors on the design being printed. Dimensional tolerance is often on the order of small feature size/resolution of the printer, though may be less.

The photopolymer resin Vorex Orange by MadeSolid and Porcelite by Tethon3D are used due to their low cost nature and characterized properties for mm-Wave applications. The layer print height was set to 50 μm for a balanced quality versus print speed compared to the 10 μm finest setting. The layers are exposed at 6500 ms and 9000 ms for Vorex Orange and Porcelite, respectively.

Silver nanoparticle inks are deposited with a Dimatix 2800 series printer. A total of two layers of the SNP ink are printed with Suntronic EMD5730 ink. Sintering occurs at 120 °C, which does not interfere with the SLA materials and there was no indication of any issues relating to coefficient of thermal expansion (CTE) between materials. With two layers of SNP ink at 120 °C, a corresponding thickness of 800 nm and a sheet resistance of 1.1 Ω/sq [5]. A roughness R_{RMS} of 100 μm was measured on the Vorex Orange substrate with a profilometer and accounted for in simulation.

The entire fabrication procedure involves printing each layer upon the next. Initially a glass carrier is attached the SLA build plate. Thereafter, photopolymer is SLA printed onto the glass. The carrier is removed from the build plate and all the uncured photopolymer resin on the build part is washed with isopropyl alcohol (IPA). At this point, inkjet printing can occur directly onto the surface of the photopolymer, followed by thermal sintering of the silver. Additional layers of photopolymer (Vorex Orange, Porcelite or more) and inks can be continually layered to desired amounts of layers, thicknesses and designs.
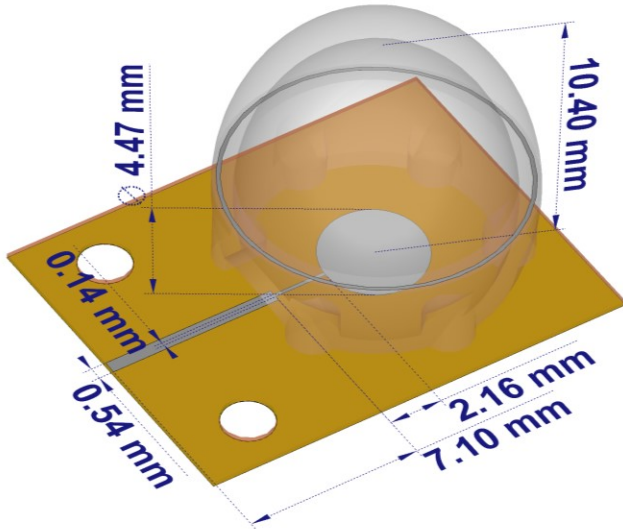

Fig. 1. 3D model of 4.46 mm and 4.19 mm major and minor axis, respectively, circular patch antenna embedded ring in the hollow elliptical dielectric lens with a microstrip of 7.1 mm and matching line length of 2.16 mm. The transparent lens is Porcelite, and the orange component is Vorex Orange. The dielectric lens has a total height of 10.40 mm and is approximately .8 mm thick. A half-circle bridge of radius 2 mm is printed above the feed line. There is a ground plane which isolates the antenna from the dies shown later.

III. CIRCULAR PATCH WITH BEAM-FORMING RING HOLLOW LENS

In order to demonstrate the multimaterial system, a right hand circular patch antenna is designed on the lower dielectric material Vorex Orange (e_r =2.65, tanδ = .017). The secondary material, Porcelite (e_r = 3.6, tanδ = .025), is used to create a more compact dielectric lens [6]. While solid high performance mm-Wave dielectric lenses have been demonstrated with 3D printing in the past [7], hollowing the dielectric lens reduces dielectric losses on the patch antenna while maintaining a similar gain to a solid lens, and is easily fabricated with 3D printing. This enables designs where lenses can be integrated directly onto substrates with reduced dielectric loading effects and reduced material costs, enabling simpler integration with existing designs. Losses in the materials may be improved as new 3D printed stereolithography materials are designed for RF applications in mind contrary to current materials that utilize lossy catalysts for improved printing performance. A conductive BFR is embedded directly into the dielectric lens, for the first time reported to the authors knowledge. This ring enhances the performance of the system by steering the main lobe, and can be used to shape the beam according to design specifications.

The substrate thickness is designed as 0.2 mm, the patch diameters are 4.46 mm and 4.19 mm for the major and minor axis of the ellipse, with a rotational angle of 57.87 degrees. The feeding line and matching line are 7.1 mm and 2.17 mm lengths with 0.54 mm and 0.14 mm widths, respectively.

$$b = a \sqrt{1 - \frac{1}{n^2}} \tag{1}$$

$$c = \frac{a}{n} \tag{2}$$

$$n = \sqrt{e_r} \tag{3}$$

The ellipsoidal geometry of the dielectric lens is defined by the relationship in formula 1-3, where a, b, c and n are the major axis, minor axis, focal length, and refractive index of the material. The elliptical hollow lens has an inner and outer ellipse. The inner and outer major axis radii are 6.10 mm and 7.04 mm, with the minor being 5.2 mm and 6 mm, respectively. The ellipses are shifted vertically so that the patch is in focus, with a shift of 3.19 mm and 3.69 mm, respectively. These values lead to a minimum wall thickness of 0.7 mm near the base and a maximum thickness at the top of 0.94 mm. The conductive ring is embedded at a height of 3.75 mm from the top of the Vorex substrate, at a radius of 5.83 mm and a width of 0.154 mm.

Additional considerations are made for bonding between layers. As seen in Fig 1, six cylinders of radius 1 mm Porcelite material along the circumference of the lens extend into the Vorex Orange dielectric to improve bonding between the two materials. A 2 mm radius bridge over the transmission line serves two purposes, it reduces any detuning effects on the

matching while also enabling the uncured material on the interior after printing to be washed and removed.

The combined elements of the system are designed to have a 10.6 dBi gain, of which 6.8 dB is realized after simulated losses of the dielectrics and silver ink.

Finally, the entire structure is printed directly with an encapsulation of four 2 mm x 2 mm die of varying heights with silver nanoparticle ink interconnects to demonstrate compatibility of direct system integration for MCM packages. The use of 3D inkjet-printed interconnects has been previously demonstrated to have low losses for thru-mold vias an offers an alternative to wire-bonding [6].
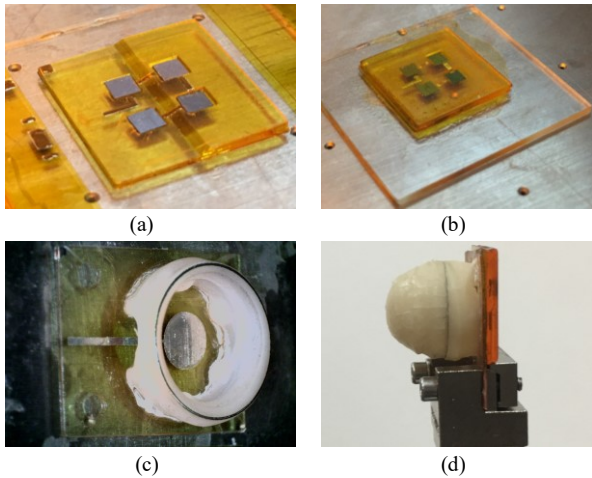

Fig. 4. (a) Dies with inkjet-printed ramps. (b) Dies encapsulated in Vorex Orange. (c) Embedded BFR in Porcelite ceramic dielectric lens, with 2 mm bridge above microstrip visible. (d) Entire printed MCM package for measurements with Southwest connector.

IV. MEASURED RESULTS

Measurements were performed on an Anritsu MS46522B VNA. The antenna exhibits a frequency shift of 0.5 GHz compared to the simulated results, with a return loss of -16.5 dB at the resonant frequency as seen in Fig 2. This variation may be due to some ink spreading on the circular patch, causing an electrically larger device, or possibly conductor losses based on additional simulations. The radiation pattern measurements are performed, which demonstrate a performance enhancement as seen in Fig 3.

V. CONCLUSION

This paper demonstrates the first of its kind multimaterial stereolithography 3D printing to enable RF devices for mm-Wave applications. The multimaterial capabilities enable variation of dielectric constants for improved design capabilities with SLA printing, and is demonstrated with the use of a higher dielectric constant hollow elliptical lens to be printed directly after a lower dielectric material. A new topology is demonstrated with an integrated BFR, which opens the way for more complex

systems integrating active electronics within dielectric lens for additional beam control. Integration of dies demonstrates that the process is compatible for integration in an active system, which will be demonstrated in future work. While material losses contribute to the performance of the system, materials are currently being developed which aim to improve performance of photopolymers in mm-Wave bands [8]–[9]. The combination of stereolithography printing and inkjet printing enable the scalability of metalized multimaterial 3D printing, while maintain low cost for the design of complex 3D topologies and offering an expanding library of materials which will enable fabrication of next generation packaging, metamaterials, filters, systems, and more.
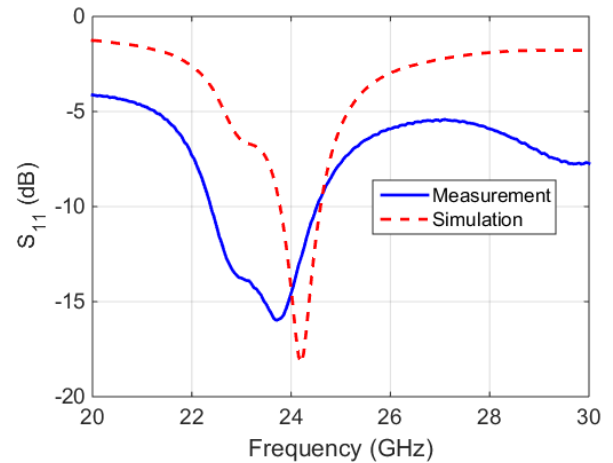

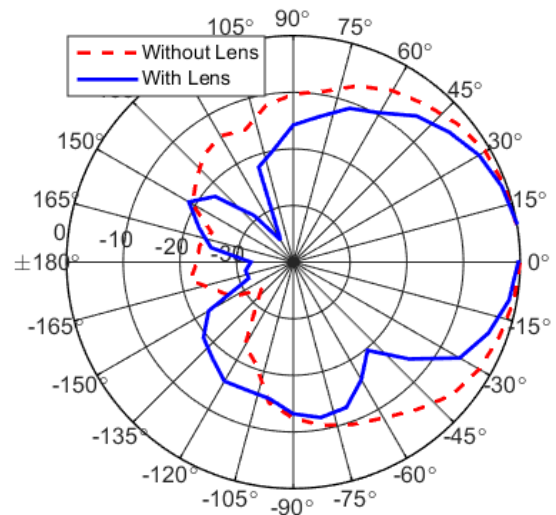Fig. 2. S11 of 3D printed circular patch antenna with beam-forming ring and simulations.

Fig. 3. Radiation pattern of the azimuth plane of simulation and measured results.

REFERENCES

[1] Joe Lopes, Amit, Eric MacDonald, and Ryan B. Wicker. "Integrating Stereolithography and Direct Print Technologies For 3D Structural Electronics Fabrication". *Rapid Prototyping Journal* 18.2 (2012): 129-143. Web. 15 Feb. 2017.

[2] C. Zhou, *et al*. "Development of multi-material mask-image-projection-based stereolithography for the fabrication of digital materials." *Annual solid freeform fabrication symposium*, Austin, TX. 2011.

[3] P. S. Kildal and S. Skyttemyr, "Dipole-disk antenna with beam-forming ring," in *IEEE Transactions on Antennas and Propagation*, vol. 30, no. 4, pp. 529-534, Jul 1982.

[4] 3D Printing Technology Comparison SLA vs DLP [Online]. Available: https://formlabs.com/blog/3d-printing-technology-comparison-sla-dlp/

[5] B. S. Cook and A. Shamim, ''Inkjet printing of novel wideband and high gain antennas on low-cost paper substrate,'' *IEEE Trans. Antennas Propag.*, vol. 60, no. 9, pp. 4148–4156, Sep. 2012.

[6] B. K. Tehrani, R. A. Bahr, W. Su, B. S. Cook and M. M. Tentzeris, "E-band characterization of 3D-printed dielectrics for fully-printed millimeter-wave wireless system packaging," *2017 IEEE MTT-S International Microwave Symposium* (IMS), Honolulu, HI, 2017, pp. 1756-1759.

[7] N. T. Nguyen, N. Delhote, M. Ettorre, D. Baillargeat, L. Le Coq, and R. Sauleau, "Design and characterization of 60-GHz integrated lens antennas fabricated through ceramic stereolithography," *IEEE Trans. Antennas Propag.*, vol. 58, no. 8, pp. 2757–2762, Aug. 2010.

[8] Deffenbaugh, Paul I., Raymond C. Rumpf, and Kenneth H. Church. "Broadband Microwave Frequency Characterization of 3-D Printed Materials". *IEEE Transactions on Components, Packaging and Manufacturing Technology* 3.12 (2013): 2147-2155. Web.

[9] M. Lis, M. Plaut, A. Zai, D. Cipolle, J. Russo, J. Lewis and T. Fedynyshyn, "Polymer Dielectrics for 3D-Printed RF Devices in the Ka Band," *Advanced Materials Technologies*, vol. 1, no. 2, pp. 160027, May, 2016.